ACS Biomaterials SCIENCE & ENGINEERING

pubs.acs.org/journal/abseba

Article

Mechanical Regulation of the Cytotoxic Activity of Natural Killer Cells

Lital Mordechay, Guillaume Le Saux, Avishay Edri, Uzi Hadad, Angel Porgador, and Mark Schvartzman*

Cite This: *ACS Biomater. Sci. Eng.* 2021, 7, 122–132

Read Online

ACCESS | Metrics & More | Article Recommendations | Supporting Information

ABSTRACT: Mechanosensing has been recently explored for T cells and B cells and is believed to be a part of their activation mechanism. Here, we investigated the mechanosensing of the third type of lymphocyte – natural killer (NK) cells, by showing that they modulate their immune activity in response to changes in the stiffness of a stimulating surface. Interestingly, we found that this immune response is bell-shaped and peaks for a stiffness of a few hundreds of kPa. This bell-shaped behavior was observed only for surfaces functionalized with the activating ligand major histocompatibility complex class I polypeptide-related sequence A but not for control surfaces, lacking immunoactive functionalities. We found that stiffness does not affect uniformly all the cells but increases the size of a little group of extra-active cells, which in turn contributes to the overall activation effect of the entire cell population. We further imaged the clustering of costimulatory adapter protein DAP10 on the NK cell membrane and found the same bell-shaped dependence to surface stiffness. Our findings reveal what seems to be "the tip of the iceberg" of mechanosensation of NK cells and provide an important insight into the mechanism of their immune signaling.

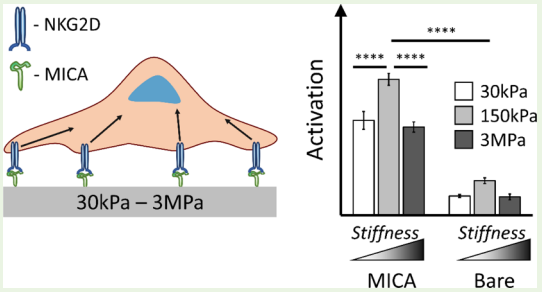

KEYWORDS: *mechanosensing, NK Cells, PDMS, receptor clustering, immune activation*

INTRODUCTION

Cells use mechanical forces to probe their environment. In the last two decades, mechanosensing and mechanotransduction have been extensively studied, mostly in the context of focal adhesions, and they are known today to play key roles in many vital cell functions, such as adhesion, proliferation, mitosis, motility, and death.[1−5] In addition, emerging studies have shed light on the role of mechanical forces in the function of immune cells.[6] Mechanistic features of the immunological synapse – a functional interface between lymphocyte and an antigen-presenting cell (APC)[7,8] – stem from actin retrograde flow, which drives the adhesion molecules and antigen receptors to form highly regulated molecular patterns.[9,10] Furthermore, it has become increasingly clear that the antigen receptors themselves, such as T cell receptors (TCRs) and B cell receptors, have mechanosensing and mechanotransductive characteristics.[11,12]

The growing evidence for the mechanical aspects of lymphocyte signaling greatly supports the emerging paradigm whereby lymphocytes use mechanical forces to discriminate between healthy and damaged cells.[13] This paradigm has been clearly demonstrated in a few recent in-vitro studies, showing that lymphocytes functionally respond to variations in the stiffnesses of the surface they contact. However, the conclusions of these studies were controversial. Some studies consistently showed an increase in the immune response, including immune activation of T cells and B cells with increasing surface stiffness,[14−17] indicating that these two cell types might share similar mechanosensing features. The substrate stiffness in these studies, however, was mostly limited to a scale of tens to hundreds of kPa. Conversely, a decrease in T cell activation with surface stiffness was reported for a stiffness range of 100 kPa to ∼2 MPa.[18] Could it then be possible that the immune response of lymphocytes to surface stiffness is bell-shaped? This question cannot be firmly addressed based on the compilation of all the above-mentioned studies, since they used cell-stimulating surfaces of different materials, different activation ligands, cells of different sources, and different experimental conditions. Each of these factors produces its own effect on cell stimulation. Hence, to address this question, the immune response of cells to the environmental stiffness must be studied for the broadest possible range of stiffnesses, while all the other parameters are kept identical. Yet, as of today, such a study has not been performed, to the best of our knowledge.

While the mechanical aspects of immune signaling have been studied mostly in T cells and B cells, much less is known

Received: July 29, 2020
Accepted: November 24, 2020
Published: December 8, 2020

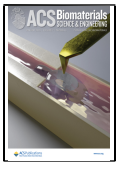

https://dx.doi.org/10.1021/acsbiomaterials.0c01121
ACS Biomater. Sci. Eng. 2021, 7, 122–132

about the role of mechanical forces in the function of the third type of lymphocytes − natural killer (NK) cells. NK cells are the sentinels of the innate immune system, and they contribute to immune protection by direct cytotoxicity, cytokine secretion, and the regulation of adaptive responses of T cells. The immune response of NK cells is regulated through a delicate balance of multiple activating and inhibitory signals.[19−21] An early indication that mechanical forces also play a role in the regulation of NK cell immune activity was recently provided by *Barda-Saad and co*, who showed that actin retrograde flow controls NK cell immune response via conformational changes of tyrosine phosphatase SHP-1.[22] Shortly afterward, we reported that NK cells stimulated onto vertical nanowires functionalized with activating ligands produced an enhanced immune response.[23] In that study, the nanowires − nanomechanical objects with an ultra-high aspect ratio and flexibility − exhibited extraordinary compliance to cellular forces as small as 10pN. We thus proposed that this high compliance produced a strong mechanical stimulus, which resulted in a much stronger degranulation compared to that of cells stimulated on a flat rigid surface. Still, the comparison between nanowires and rigid surfaces represents two extreme cases. NK cells interact in-vivo with a diverse activating environment, including relatively soft myeloid, monocyte, and dendritic cells whose stiffness ranges within hundreds to thousands of Pa,[24] and stiffer ECM and tumor cells and tissues the stiffnesses of which reached almost to 100 kPa.[25,26] In addition, NK cells are activated in-vitro for immunotherapeutic properties,[27] in an environment much harder than the physiological one. It was recently shown that modulating the stiffness of the activating environment can control in-vitro activation of T cells,[28,29] proving an intriguing perspective for designing novel materials for improving immunotherapy that can be also used with NK cells. Thus, the nature of mechanical interactions between NK cells and their environment should still be systematically studied for the widest possible range of mechanical and biochemical stimuli, individually and in combination with each other.

In this work, we carried out the first, to the best of our knowledge, systematic study of the immune response of NK cells to the stiffness of their environment. For this purpose, we stimulated primary NK cells onto elastic surfaces whose stiffnesses varied from 30 kPa to 3 MPa. This range, which spans two orders of magnitude, encompasses most of the ranges previously used to study T cells and B cells. In order to provide NK cells with biochemical stimulation, we functionalized these surfaces with major histocompatibility complex (MHC) class I polypeptide-related sequence A (MICA) molecules that are specifically recognized by the NK cell activating receptor NKG2D.[30] We assessed the immune response of NK cells to the surface stiffness via surface expression of lysosomal-associated membrane protein-1 (CD107a) and found that it was nonlinear and had a bell-shaped characteristic with a peak at 150 kPa. To separately assess the effect of each stimulus − mechanical and chemical − we interfaced NK cells with control surfaces that had no bioactive functionalities and found that these control surfaces yielded relatively low degrees of activation, whose dependence on surface stiffness was negligible. We also quantified the spreading of the stimulated NK cells and found that it does not correlate with their immune activity. Concurrently, we found that a surface stiffness of 150 kPa stimulated the formation of the highest number of clusters of DAP10 − an adaptor protein of the NKG2D receptor, indicating that the enhanced activation for this surface stiffness is associated with NKG2D organization and signaling. Overall, these results reflect the existence and importance of mechanosensing in NK cells and provide an intriguing insight into their nonlinear response to the physical features of their environment.

MATERIALS AND METHODS

Sample Fabrication and Biofunctionalization. Elastic surfaces of polydimethylsiloxane (PDMS) were prepared using a standard elastomer kit Sylgard 184 (Dow Inc.), with different hardener−resin ratios of 1:50, 1:35, and 1:10 (w/w).[31] The mixture was poured onto a glass slide and smeared, to achieve a PDMS thickness of ∼0.3 mm.[32] Finally, the PDMS samples were degassed in a desiccator and cured for 1 h at different temperatures: 130 °C for 1:50 and 1:35 ratios and 200 °C for the 1:10 ratio.[33] The elastic modulus was assessed from force−distance curves of contact mode AFM (Asylum Research, MFP-3D-Bio, Hertz model,[17,34,35] see the Supporting Information for details). To functionalize PDMS surfaces with MICA ligands, the samples were first treated in oxygen plasma for 5 s (Harrick PDC-32G) and then modified with (3-aminopropyl) triethoxysilane (APTES) by immersing into 10% APTES solution (Sigma-Aldrich) in ethanol for 10 min, rinsing with ethanol, and drying for 10 min in an oven at 80 °C.[36] Then, the samples were incubated overnight at 4 °C in 2 μg/mL with a solution of His-MICA (SinoBiological) in phosphorus buffer solution (PBS).

Immunofluorescence Characterization of PDMS Functionalization. Fluorescence microscopy was used to confirm that MICA was efficiently immobilized onto APTES-functionalized PDMS. For this purpose, MICA was labeled with a red fluorophore as follows. A 1:50 v/v of 5(6) carboxytetramethyl-rhodamine N-succinimidyl ester (TAMRA−NHS) was added to 10 μL of MICA with 5 μL of $NaHCO_3$ and 34 μL of PBS. The mixture was left to react for 1 h. The mixture was purified using a protein purification kit (Life technologies). APTES-functionalized PDMS was then immersed in the TAMRA−MICA solution overnight at 4 °C in 2 μg/mL. Afterward, we then rinsed the samples once with PBS and once in pure water and mounted them on a coverslip with the DAKO fluorescence mounting medium (Agilent). The samples were imaged with an epifluorescence microscope (Nikon Eclipse Ti2-E). Please see the Supporting Information for more details.

Isolation of Primary NK (pNK) Cells. Cells were isolated using a human negative selection-based NK isolation kit (RosetteSep, STEMCELL Technologies). Purified NK cells were then cultured in a stem cell growth medium (CellGenix GMP SCGM, 20802−0500) supplemented with 10% heat-inactivated human AB plasma from healthy donors (SIGMA, male AB, H-4522), 1% l-glutamine, 1% Pen-Strep, 1% sodium pyruvate, 1% MEM-Eagle, 1% HEPES 1 M, and 300 IU/mL recombinant human IL-2 (PeproTech). pNK cells were purified from the peripheral blood of healthy, adult, volunteer donors, recruited by written informed consent, as approved by the Institutional Review Board Ben-Gurion University of the Negev (BGU).

NK Cell Activation Experiments. Cultured pNK cells were seeded onto the surfaces in an amount of 1 million cells per sample in a fresh medium (containing 50 U/mL IL2) prepared from SCGM and RPMI (1:6 v/v) supplemented with APC antihuman CD107a (1:1000 v/v). The cells were incubated for 3 h on the surfaces at 37 °C. After the incubation, the surfaces were rinsed once in PBS, fixed with 4% paraformaldehyde for 10 min at 4 °C, rinsed once again in PBS, and then stained directly with Alexa Fluor 555 phalloidin (Life Technologies) diluted 1:40 v/v in a blocking buffer (5% skim milk in PBS) without permeabilization for 1 h at 37 °C to prevent damage to the cell membrane. Finally, the samples were rinsed once with PBS and once in pure water, and then, the nuclei were stained by mounting the samples on coverslips with a Fluoroshield mounting medium with DAPI (Abcam) to prepare the samples for imaging. NK cells were imaged using a Nikon eclipse Ti2-E epifluorescence microscope system (20x Ph1 DLL air objective, wavelengths of 365,

https://dx.doi.org/10.1021/acsbiomaterials.0c01121
ACS Biomater. Sci. Eng. 2021, 7, 122−132

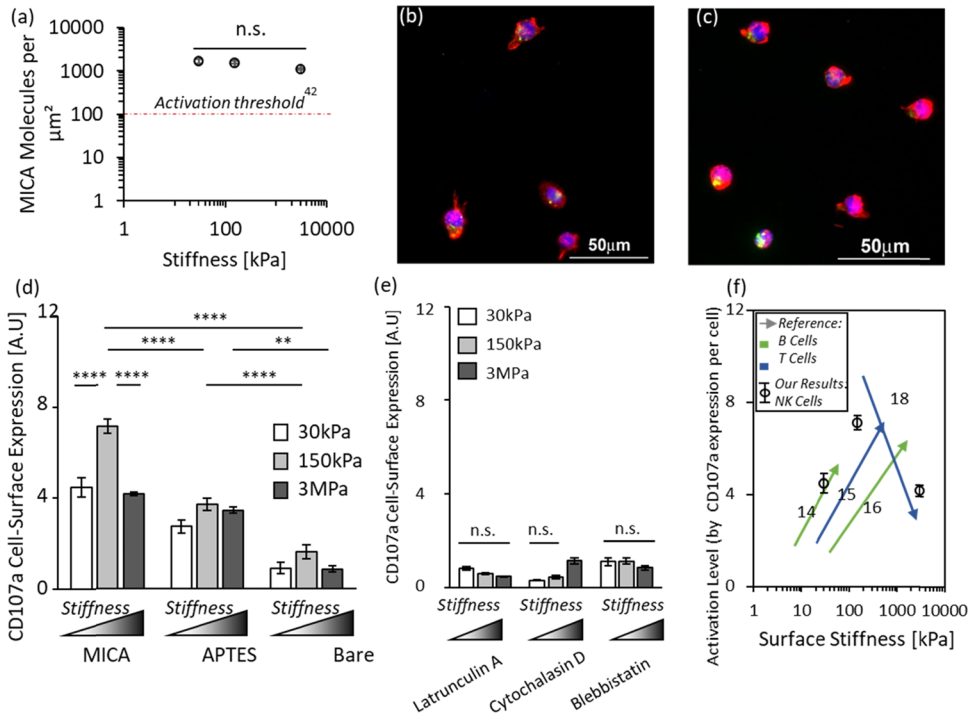

Figure 1. (a) TAMRA−MICA density vs surface stiffness of PDMS. (b, c) Representative images of NK cells on MICA-functionalized PDMS with stiffnesses of 30 kPa and 3 MPa, respectively. The cytoskeleton was stained with phalloidin (red), nucleus, with DAPI (blue), and CD107a, with its fluorescently labeled mAb (green). Activation threshold (red dashed line) is based on the previously established minimal surface density of MICA needed for the stimulation of NK cells.[42] (d) Degree of CD107a cell-surface expression of NK cells on MICA-modified, APTES-modified, and bare PDMS, respectively. The degree of CD107a was quantified by summarizing the fluorescence intensity of the APC-labeled anti-CD107a per cell (for ease of view, the APC-labeled anti-CD107a was pseudo-colored in green in b−c). The results show the compilation of at least 200 cells from at least three different experiments and for at least three sets of samples per experiment. Using GraphPad Prism, analysis of variance and Tukey's post hoc tests were performed to assess the significant changes in behavior − four stars (****) represent $p < 0.0001$. (e) Degree of CD107a cell-surface expression of NK cells on MICA, when NK cells were treated with latrunculin A, cytochalasin D, and blebbistatin. The degree of CD107a was quantified by summarizing the fluorescence intensity of the APC-labeled anti-CD107a per cell. The results show the compilation of more than 20 cells per sample. Using GraphPad Prism, analysis of variance and Tukey's post hoc tests were performed to assess the significant changes in behavior of $p < 0.05$. (f) Compilation of activation trends reported for T cells and B cells is shown by arrows with the corresponding reference numbers, and our results for NK cells are shown in circles.

550, and 635 nm for DAPI, Alexa Fluor 555 and CD107a, respectively). Please see the Supporting Information for details on the methodology used to quantify CD107a expressions.

Imaging DAP10 Clustering. pNK cells were seeded on the surface for 10 min and fixed according to the protocol described in the previous section, excluding the anti-CD107a supplement. After permeabilization (Triton X-100, 0.1% in PBS, 15 min at 4 °C), the cells were incubated for 1 h at 37 °C in blocking buffer and then for another 1 h with Alexa Fluor 488 phalloidin (Life Technologies, 1:40 v/v in blocking buffer) and Alexa Fluor 594 labeled antihuman DAP10/HCST (R&D Systems, 1:500 v/v in blocking buffer) to stain the cytoskeleton and DAP10 clusters, respectively. Finally, the samples were rinsed once with PBS and once in pure water, and then, the nuclei were stained by mounting the samples on coverslips with the Fluoroshield mounting medium with DAPI (Abcam) to prepare the samples for imaging. DAP10 clusters were characterized using a Zeiss LSM880 confocal microscope system equipped with an Airyscan detector for superresolution microscopy (63 × 1.4 NA DIC M27 oil objective, wavelengths of 405, 488, and 561 nm).[37] Please see the Supporting Information for more details.

RESULTS AND DISCUSSION

NK Cells Produce a Bell-Shaped Response to the Substrate Stiffness. In order to find out whether and how NK cells modulate their immune activation in response to the environmental stiffness, we prepared elastic surfaces of PDMS with variable elastic moduli − 30 kPa, 150 kPa, and 3 MPa. We experimentally confirmed the elastic moduli of the obtained PDMS substrates using AFM (Figure S1a). To add a biochemical stimulus to the PDMS surfaces, we functionalized the PDMS with MICA ligands. For this purpose, we first functionalized the PDMS with APTES, which facilitates the physisorption of biomolecules via electrostatic interactions.[38] In this manner, we produced a layer of physisorbed MICA, which was known to effectively engage NK cell receptors.[39]

We confirmed that MICA was efficiently immobilized onto APTES-functionalized PDMS by incubating these surfaces in an aqueous solution of TAMRA-labeled MICA and imaged the obtained surfaces using an epifluorescence microscope. The strong contrast in fluorescence emission between the TAMRA−MICA functionalized surface and APTES-functionalized surfaces (Figure S2a,b) confirms the effective chemisorption of MICA. To ensure that the elastic modulus is the only parameter that is changed between different samples and the stimulating conditions are not affected by the difference in the amount of MICA, we quantified the surface density of MICA molecules for each stiffness of PDMS (see the Supporting Information). To do so, we first assessed the fluorescent signal of a known quantity of TAMRA-labeled MICA (Figure S2c) and used it as a calibration factor to assess the surface density of MICA on our different surface stiffnesses of PDMS samples. We found that this surface density was quite

https://dx.doi.org/10.1021/acsbiomaterials.0c01121
ACS Biomater. Sci. Eng. 2021, 7, 122−132

similar for all the samples, ranging between 1100 and 1700 molecules per square micron (Figure 1a). We believe that the slight differences in the MICA concentration stem from different degrees of crosslinking in PDMS, which modify its surface porosity, and, as a consequence, the degree of APTES physisorption.[40] Given the fact that MICA has a diameter of about 12 nm,[41] we can deduce that MICA was immobilized onto the PDMS surface in an almost closely packed configuration. Furthermore, the obtained density of MICA is far above the minimum density required for NK cell activation, which is about ∼100 molecules per square micron.[42] Therefore, we created here a stimulation environment for NK cells with the maximum possible amount of biochemical stimulus, while the mechanical stimulus, which is defined by the surface stiffness, was the only variable. Importantly, we verified that neither plasma treatment nor functionalization modified the surface stiffness of PDMS (Figure S1b). We also verified the stability of MICA functionalization by incubating it for 3 h in the cell culturing medium at 37 °C and comparing its fluorescent intensity with that of freshly immobilized MICA (Figure S2d,e). Importantly, the images in Figure S2d show that the distribution of immobilized MICA is very uniform and that this distribution itself cannot produce any driving forces that may affect the cell behavior.

We incubated primary NK cells on the elastic surfaces for 3 h. In order to elucidate separately the effect of chemical and mechanical stimulations on NK cell immune response, we used two types of control surfaces: PDMS functionalized with APTES but without MICA and bare PDMS. We quantitatively assessed the degree of immune activation of NK cells by imaging the surface expression of the lysosome-associated membrane protein-1 (CD107a), which is a common degranulation marker.[43,44] Notably, it takes at least 2 h of stimulation of NK cells for CD107a expression that correlates NK cell-mediated lysis of target cells.[44] Here, 3 h of incubation time was chosen to ensure the complete expression of CD107a and its labeling. To image CD107a, we added fluorescently labeled anti-CD107a to the incubation medium. After incubation, we fixed and stained the cells with phalloidin and DAPI for the cytoskeleton and nucleus visualization, respectively. We quantified the activation degree of NK cells on each tested surface by measuring the average signal produced by the CD107a antibody, which had accumulated at the cell surface.

Figure 1b,c shows representative images of NK cells stimulated on MICA-functionalized PDMS with the moduli of 30 kPa and 3 MPa, respectively. CD107a accumulated on the cell membrane and stained with its fluorescent antibody appears in bright green. Figure 1d shows the average signal of CD107a per cell on MICA-functionalized surfaces and on the control surfaces. As expected, MICA−PDMS stimulated a significantly higher CD107a expression of NK cells compared to that obtained for the control surfaces. Furthermore, CD107a expression on MICA−PDMS greatly varied with stiffness, and this variation was nonlinear and bell-shaped, with a maximum CD107a signal for 150 kPa. On the other hand, on the control surfaces, the effect of surface stiffness on the CD107a expression was significantly less pronounced. This result largely mirrors our previous report on the activation of NK cells on nanowires, where NK cells showed significant activation only on nanowires functionalized with MICA, while control surfaces lacking either nanowires, MICA, or both, did not induce a substantial activation of NK cells.[23] To verify that the difference in activation does not stem from a slight variation in MICA surface concentration between the samples, we produced a controlled experiment in which we compared the activation of NK cells on two surfaces with the same stiffness − 150 kPa, which had surface MICA concentrations of 200 molecules per μm^2 and 1000 molecules per μm^2. Notably, MICA concentration in both samples was above the threshold we previously established for an effective NK cell activation.[42] Despite the 5-fold difference in MICA surface concentration, both samples produced a similar level of activation, which was higher compared to that on bare PDMS with the same stiffness (Figure S2f). Based on this result, we deduce that the difference in NK cell activation presented in Figure 1d stems only from the difference in PDMS stiffness. To further verify that NK cells indeed sensed the stiffness of the stimulating substrates, we treated them with actin inhibitors latrunculin A[45] and cytochalasin D,[46] as well as with myosin inhibitor blebbistatin.[47] All the treatments largely reduced the degree of degranulation on MICA-covered PDMS (Figure 1e) and bare PDMS (Figure S3) and abrogated the sensitivity of the cells to the difference in the stiffness.

The observed bell-shaped response of NK cells to stiffness is highly intriguing, and its exact mechanism is yet to be understood. Importantly, this is the first time, to the best of our knowledge, that the immune response of NK cells to variations in environmental stiffness has been systematically studied. However, it could be of interest to compare the observed behavior of NK cells to that of other lymphocytes stimulated in analogous conditions. As mentioned above, the effect of surface stiffness on immune activation was previously reported for T cells and B cells, but those reports used relatively short ranges of surface stiffnesses and showed different stiffness versus activation trends that appeared to depend on the studied stiffness range.[14−16,18] As previously stated, the combination of those studies for T cells suggested the possibility of a bell-shaped correlation.[6] While this possibility should be separately verified in the future for T cells and B cells, our result mirrors the state-of-the-art studies (Figure 1f) and shows that at least for NK cells, the bell-shaped immune response to stiffness does indeed exist.

As anticipated, bare PDMS surfaces produced the lowest immune activation of NK cells, due to the absence of any chemical stimulus. Still, the effect of the surface stiffness of bare PDMS is also bell-shaped, although it is not well-pronounced. These results highlight the need for a chemical stimulus to allow lymphocytes, such as NK cells, to mechanically sense their environment and transduce this sensing into a functional immune response. In addition, APTES-functionalized surfaces stimulated a higher immune response compared to bare PDMS. Here, the effect of surface stiffness was negligible. We presumed that APTES stimulated NK cell activation due to the positive charges of the terminal amino groups, which produce asymmetric charge distribution across the cell membrane, and might positively affect NKG2D signaling, similar to that of TCRs in T cells.[48] Still, the activation on APTES-functionalized surfaces was uniform for all the tested stiffnesses. This suggests that APTES-induced activation, regardless of its exact nature, is independent of the mechanical stimulus provided by the surface stiffness and can neither diminish nor enhance the latter, as biochemical activation induced by MICA does.

Stiffness of Antigen-Functionalized Surfaces Regulates the Adhesion of NK Cells. We next focused on

https://dx.doi.org/10.1021/acsbiomaterials.0c01121
ACS Biomater. Sci. Eng. 2021, 7, 122−132

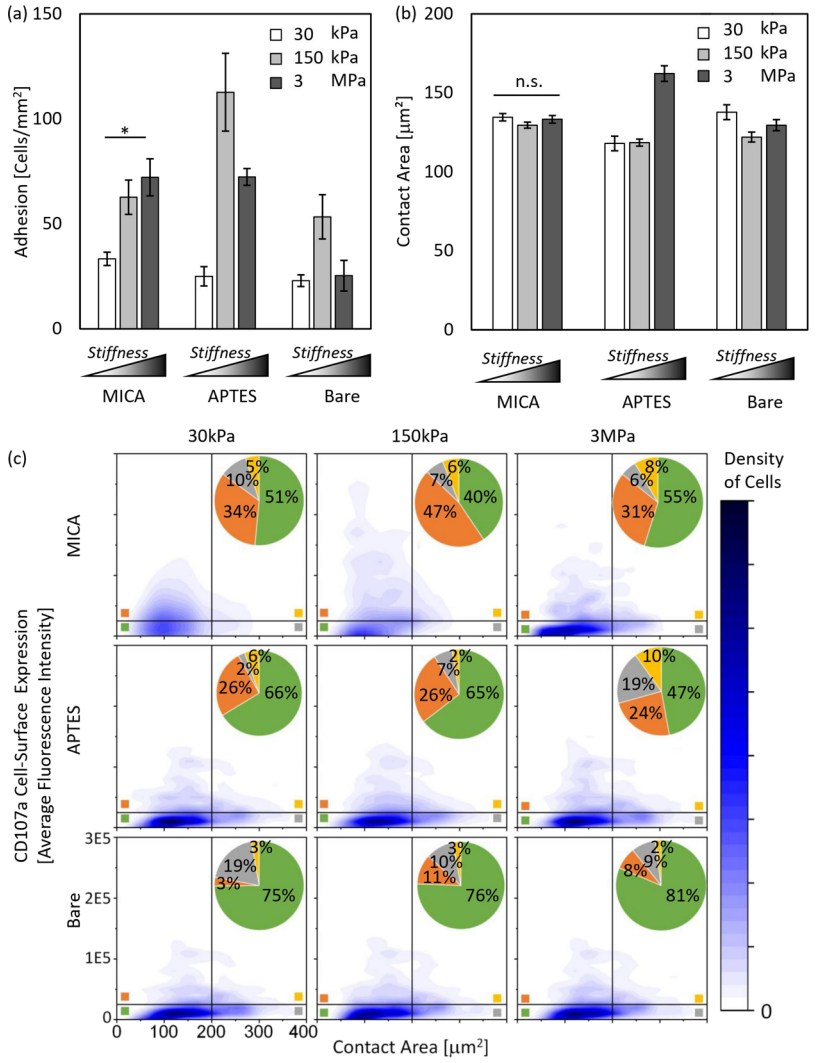

Figure 2. (a) NK cell adhesion vs stiffness. Cell adhesion was calculated by counting the projected contact area of the cell cytoskeleton divided by the area of the surface that they adhere to, for each type of sample. (b) NK cell spreading vs stiffness. Cell spreading was quantified by measuring the projected contact area of the cell cytoskeleton, for each type of sample. The results show the compilation of at least 200 cells from at least three different experiments and for at least three sets of samples per experiment. Using GraphPad Prism, analysis of variance and Tukey's post hoc tests were performed to assess the significant changes in behavior − one star (*) represents $p < 0.05$. (c) Density plots of spreading (defined by contact area) vs activation (defined by the degree of CD107a). Percentages of cells for each of the four subpopulations are shown in the inset. The results are shown the compilation of at least three different experiments and for at least three sets of samples per experiment. The plots are analyzed using Origin software.

whether and how the surface stiffness and biochemical functionalization affect the adhesion of NK cells. Importantly, our PDMS surfaces had no specific adhesion functionalities that can stimulate adhesion mediated by NK cell adhesion receptors, such as intercellular adhesion molecule 1 (ICAM), but only MICA, which engages NKG2D receptors. We estimated the degree of adhesion by counting the number of cells per unit area after mounting the samples for imaging (Figure 2a). The adhesion and its dependence on surface stiffness varied between the probed surface chemistries. As expected, bare PDMS surfaces yielded the lowest degree of adhesion, due to a lack of any biochemical functionalities that specifically recognize NK cell receptors. Surprisingly, for MICA-functionalized surfaces, we obtained a consistent increase in the degree of cell adhesion with an increase in surface stiffness. Conversely, the control surfaces (both bare PDMS and APTES-functionalized PDMS) produced an NK cell adhesion bell-shaped tendency with increasing surface stiffness. The relatively high adhesion observed on APTES−PDMS can be explained, again, by its positive charges.[49] To eliminate any ligand-independent effects and demonstrate the necessity of MICA for the effective activation of NK cells, we added two more control samples of 150 kPa in which two mock proteins with inert activities, small ubiquitin-like modifier (SUMO) and IgG2a, were immobilized instead of MICA and verified that the cell response was similar to that on the APTES surface, (Figure S4). Our results indicate that specific and nonspecific functionalities signal via different pathways and that their signals, while integrated with the mechanical signals produced by the surface stiffness, affect cell adhesion differently. Although the mechanism of this integration has to be further studied, we can conclude at this stage that we established an experimental toolbox that can independently control the adhesion of NK cells via either biochemical stimuli produced by the chemical functionalities or mechanical stimuli produced by the surface elastic modulus.

https://dx.doi.org/10.1021/acsbiomaterials.0c01121
ACS Biomater. Sci. Eng. 2021, 7, 122−132

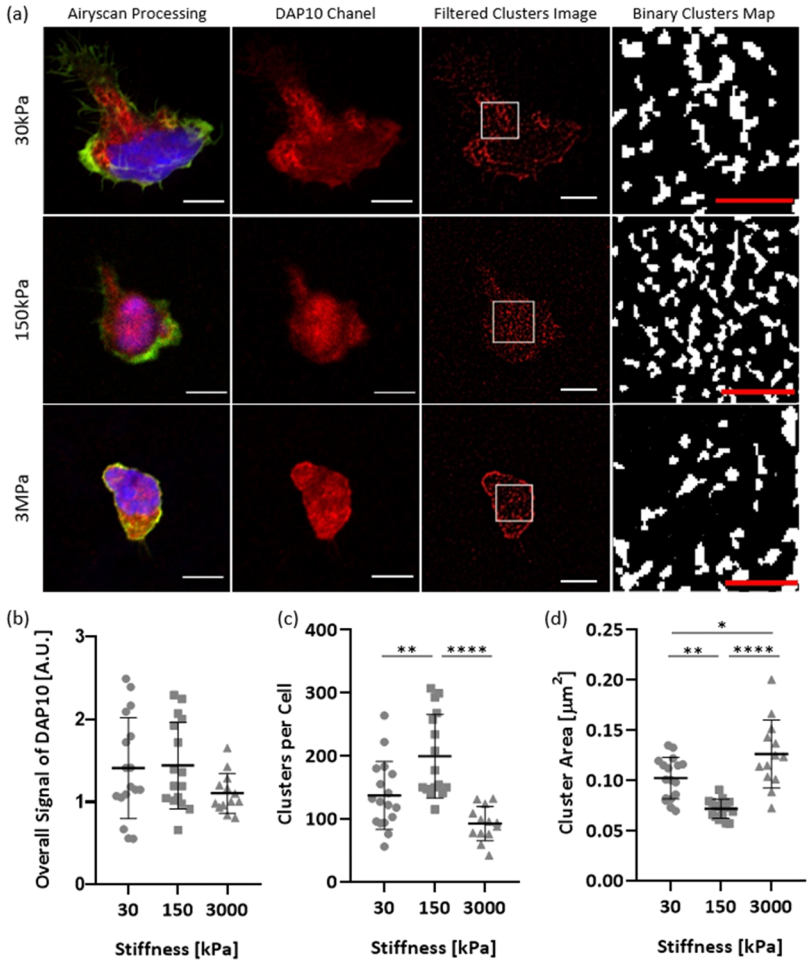

Figure 3. Clustering of NKG2D. (a) Representative images of NK cells on MICA-functionalized PDMS with stiffnesses of 30 kPa, 150 kPa, and 3 MPa, respectively. The cytoskeleton was stained with phalloidin (green), nucleus, with DAPI (blue), and DAP10, with its fluorescently labeled (red). White scale bar − 5 μm; red scale bar − 2 μm. Clustering of NKG2D for each PDMS sample with stiffnesses of 30 kPa, 150 kPa, and 3 MPa is shown in (b) overall signal of DAP10 per cell, (c) density of clusters per cell, and (d) average cluster area per cell. The results show the compilation of more than 10 cells per sample. A minimum of 50 clusters were analyzed per cell. Using GraphPad Prism, analysis of variance and Tukey's post hoc tests were performed to assess the significant changes in behavior − four stars (****) represent $p < 0.0001$.

Stiffness of the Antigen-Functionalized Surface Does Not Affect NK Cell Spreading but Regulates the Number of Highly Activated NK Cells. It was previously shown that the spreading of NK cells does not necessarily require interaction with adhesion functionalities LFA-1 but can occur via MICA ligation, which, however, produces a cell morphology different from that induced by LFA-1 ligation.[50] Furthermore, we recently showed that NK cell spreading depends on the spatial density of MICA ligands and that at least 100 molecules of MICA ligands per square micron are required to stimulate the full spreading of NK cells.[42] Still, all the above studies were done on rigid glass surfaces coated with ligands, and the role of surface stiffness in the spreading of NK cells has not yet been explored.

Here, we assessed the impact of stiffness on the spreading of NK cells, by measuring their projected area after 3 h of incubation (Figure 2b). We found that in the case of MICA-functionalized PDMS, surface stiffness had no effect on NK cell spreading. This finding mirrors the previously reported lack of correlation between the spreading and the activation of NK cells.[51] Conversely, APTES functionalization stimulated higher spreading on stiffer PDMS.

We also examined whether there is a correlation between the spreading and activation degree. To this end, for each set of stimulation conditions (i.e., stiffness + chemistry) we divided cells into four subpopulations defined by spreading and activation gates. The values for the spreading and activation gates for the 2D spreading−activation density plots (Figure 2c) were determined using the average + standard error of the cell areas and CD107a signals for bare PDMS. It can be seen from the 2D spreading−activation density plots (Figure 2c) that for most of the stimulating conditions, the distribution between the populations was very similar, and thus, the plots had almost identical outlines. For these outlines, more than half of the cells can be included in the category, which is defined by low spreading and low activation, while a relatively low percentage of cells showed either high activation or high spreading, and a negligible percentage of cells showed both.

A clear exception in the spreading−activation plot is for 150 kPa PDMS functionalized with MICA, which induced the highest average degree of degranulation, as shown in Figure 1d. In this plot, we observed an exceptionally high fraction (>50%) of NK cells defined as "highly activated" by our "activation threshold". Surprisingly, the vast majority of these highly activated NK cells (47% out of a total of 54%) were less

https://dx.doi.org/10.1021/acsbiomaterials.0c01121
ACS Biomater. Sci. Eng. 2021, 7, 122−132

spread, i.e., below the "spreading threshold". Indeed, *Culley* et al. recently demonstrated that the extent of spreading for NK cells is not proportional to the outcome of signaling balance in NK cells but rather occurs if a threshold of activation is surpassed.[50] This lack of direct proportionality between spreading and immune activation, especially when estimated after a relatively long time of incubation, is observed for all the combinations of surface stiffness and surface chemistry presented herein but is more pronounced for 150 kPa PDMS functionalized with MICA.

What also follows from the spreading−activation plots of 150 kPa PDMS functionalized with MICA and from its comparison to other conditions is that the high activation on 150 kPa MICA−PDMS (Figure 1d) stems not from a uniform increase in the activation in all the cells but from an increase in the subpopulation of highly activated cells, while the cells outside this subpopulation retain their low activation level. One possible explanation for this observation can be based on the fact that NK cells are divided by several subpopulations based on their cytotoxic activity.[51] Indeed, it was recently reported that individual NK cells placed in microwells together with target cells could be categorized into subpopulations by their cytotoxic response, e.g., the number of killed target cells,[51] and that there was a small but extremely active subpopulation of NK cells, which was called "serial killer" NK cells, due to their ability to eliminate a number of target cells each.[52] This in-vitro detection of the "serial killer" population mirrors a prevalent model by which only a minority of NK cells is responsible for tumor elimination. The existence of subpopulations with different cytotoxic activities can be related to the fact that NKG2D expression varies among cells (Figure S5). Thus, the highly active cells are presumably those expressing larger amounts of NKG2D. While the percentage of extra-active NK cells was initially the same for all the tested samples, we showed that by tuning the mechanical elasticity of the stimulating environment, the relative fraction of extra-active NK cells that undergo degranulation can be controllably manipulated, and the change in this fraction affects the average activation level of the entire population of NK cells. Therefore, the mechanical signaling provided by PDMS does not evenly increase the immune activity of the entire population of NK cells but rather increases the fraction of NK cells that overcome a certain activation threshold.

The Effect of the Surface Stiffness on the Activation of NK Cells Is Associated with the Receptor Microclustering. Organization and clustering of receptors within the membrane of lymphocytes are the key factor in their activation.[53,54] The cytotoxic activity of NK cells is tightly regulated by the microclustering of their activating receptors such as CD16,[55] NKG2D,[56] and NKP46[57] as well as of their inibitory receptors such as KIR2DL1.[58] This microclustering can be regulated in-vitro by various micro/nanoplatforms with the controlled spatial distribution of activating and inhibitory ligands.[59−62] On the other hand, it was natural to wonder whether surface stiffness controls the cytotoxic activity of NK cells by modulating the clustering of target receptors of the used activating ligands or via a signaling pathway independent of receptor clustering. Since binding NKG2D to MICA could prevent its availability for a fluorescent antibody, we did not stain NKG2D directly. Instead, we labeled its transmembrane adaptor DNAX-protein 10 (DAP10), whose hexametric complex with NKG2D activates signaling in NK cells[63,64] and therefore has the proximity of few nanometers to the NKG2D receptor.[39] Furthermore, the colocalization of NKG2D and DAP10 clusters was recently demonstrated at the nanometric scale within the membrane of activated NK cells.[39] Notably, receptor clustering is an early signaling event, and NK cells were reported to form mature DAP10 clusters at the cell membrane within a few minutes.[39] Thus, to quantify DAP10 clustering, we imaged the cells after 10 min of incubation.

The clusters of DAP10 were imaged using a Zeiss LSM880 confocal microscope equipped with an Airyscan detector for superresolution microscopy.[37] We analyzed DAP10 clustering using ImageJ by identifying clusters and measured their density per cell and their size (see the Supporting Information for details). Figure 3a shows typical microclusters of DAP10 in NK cells stimulated on the MICA-functionalized surface with stiffnesses of 30 kPa, 150 kPa, and 3 MPa and the quantification of cluster density and cluster size. We found that the total amount of DAP10 adaptor protein expressed by NK cells was similar for all the tested surfaces (Figure 3b). On the other hand, we found that surface stiffness altered the way DAP10 receptors are clustered within the cell membrane. The highest density of clusters per cell and concurrently the smallest clusters was found in cells cultured on MICA-functionalized PDMS with a stiffness of 150 kPa (Figure 3c,d). Notably, it is possible that the data on cluster size include an artifact of the point spread function of confocal microscopy, which might enlarge the observed cluster size versus the real one. Indeed, superresolution microscopy using the dSTORM method demonstrated nanocluster organization of NKG2D−DAP10 on the surface of activated NK cells.[57] However, regardless of the uncertainty in the absolute cluster size, we concluded that the cluster size has valley-shaped dependence on environmental stiffness, at least qualitatively, and has a minimum of 150 kPa in our experiments. Moreover, the resolution limitations of the used microscopy method do not affect the reliability of the obtained density of clusters per cell versus surface stiffness, whose trend mirrors the already familiar bell-shaped behavior observed for NK cell activation, with a peak at 150 kPa.

These results strongly suggest a correlation between surface stiffness-regulated NK cell activation and the clustering of DAP10 adaptors and most probably its associated activating receptors NKG2D, although the latter was not directly imaged. Indeed, the obtained correlation between the activation of NK cells and clustering of DAP10 mirrors similar correlation recently reported by Bálint et al.[39] There, the effect of different ligands on the activation of NK cells was studied, and it was found that MICA not only stimulated the highest degranulation but also stimulated the organization of NKG2D into more numerous and smaller clusters. Notably, in that work, the ligands were immobilized onto a rigid surface, and the biochemical stimulus provided by MICA was the only environmental parameter through which activation was controlled. Thus, while receptor clustering is undoubtedly the key factor in the regulation of NK cell cytotoxic activity, this factor itself can be regulated either biochemically via antigens or physically via mechanical properties of the environment. The final outcome, i.e., activation, is produced by the cumulative effects of the biochemical and physical stimuli.

The exact mechanism by which environmental stiffness regulates receptor clustering in NK cells and therefore their activation remains unclear. One probable scenario is based on

https://dx.doi.org/10.1021/acsbiomaterials.0c01121
ACS Biomater. Sci. Eng. 2021, 7, 122−132

the possibility that NKG2D receptors sense mechanical forces and transduce mechanical signals via conformational changes. Such a mechanosensing mechanism has been recently established for TCRs in T cells[65] and depicts the TCR−pMHC complex as a "catch-bond", the lifetime of which increases with the applied force up to a peak of ∼10pN[66] and then decreases when the force is further increased. The catch-bond characteristics of the TCR−pMHC complex were explored experimentally using optical tweezers,[67] micropipette-based adhesion assays,[68] and a biomembrane force probe.[66] These characteristics were also modeled in terms of TCR and membrane conformation.[69] This catch-bond mechanism has also been observed in NK cells for the activating receptor CD16,[70] but not yet for NKG2D. Notably, the fact that the pronounced bell-shaped response was observed only for MICA-coated surfaces, together with the well-established specificity of NKG2D−MICA binding,[30] indicates that this response is associated with NKG2D signaling. Thus, a suggested scenario by which NKG2D forms a catch-bond with MICA could explain the observed bell-shaped effect of the stiffness of MICA-functionalized surfaces on the receptor clustering and on the immune response of NK cells (Figure S6a,b). Since MICA is electrostatically tethered to the elastic surface, both the surface and the NKG2D−MICA complex can be considered as two independent elastic components interconnected in series. While the NKG2D−MICA complex moves toward a cluster formed by other NKG2D molecules, each elastic component deforms, and the deformation of each component depends on their relative spring constants. If the surface is relatively soft (Figure S6b left), it would contribute to most of the deformation, while the NKG2D−MICA complex would stay in its "loose" state. This scenario corresponds to the left part of the force versus life-time bell-shaped curve. With an increase in surface stiffness, the deformation between the two components is distributed more evenly, and the catch-bond reaches its optimal conformation and therefore the longest lifetime, which corresponds to the peak of the curve (Figure S6b middle). A further increase in surface stiffness induces a deformation that cannot be withstood by the bond, which eventually breaks (Figure S6b right). Again, the observed functional response of NK cells to the variation of surface stiffness can be at most an indirect indication that the NKG2D−MICA complex is indeed a catch-bond. The direct demonstration of the catch-bond behavior of the NKG2D−MICA complex should be done to support the proposed model, similar to the above-mentioned studies on TCR−pMHC agonist the catch-bond.

CONCLUSIONS

In summary, our paper provides new insight into the diversity of environmental stimuli for NK cells and demonstrates their effects, separately and in combination with one other, on NK cell activation. Among these stimuli, the biochemical ones have been the most broadly studied so far. In contrast, physical stimuli are still far from being fully explored. Here, we not only provided the first direct evidence that NK cells sense the stiffness of the surface they contact but also revealed the trend with which this stiffness affects their immune response. This trend mirrors the compilation of recent studies on T cells and indicates that both types of cells have similar mechanosensing characteristics. Remarkably, our conclusions are based on three stiffnesses, yet much could happen between 150 kPa and 3 MPa. Assessing NK cell response to a larger number of stiffnesses within this range will reveal a more detailed mechanism of NK cell mechanosensitivity, and this is the subject of our follow-up study. The observed bell-shaped response to surface stiffness shows that there is an optimal range of stiffness for NK cell stimulation, and NK cells likely utilize their ability to sense the stiffness in their decision making as to whether a target cell should be attacked or tolerated. The correlation between the bell-shaped immune response to stiffness and the bell-shaped dependence of receptor clustering indicates that these receptors are involved in mechanosensing and probably act as mechanotransductors. The proposed catch-bond mechanism of NKG2D−MICA can explain the observed bell-shaped response but still needs to be verified. Also, we employed here a reductionist stimulating platform, the chemical stimulus of which included only activating ligands unlinked to the cytoskeleton. Thus, surface stiffness cannot directly affect cytoskeleton rearrangement, which is known to play a critical role in the formation of the immune synapse. Follow-up studies will involve ICAM-mediated adhesion of NK cells, to incorporate this important aspect of mechanostimulaiton. Finally, studies of physical signaling in lymphocytes thus fat focused mostly on the effect of the environmental stiffness. Yet there has been increasing evidence of many additional physical factors that regulate the immune function of cells. For example, it has recently been shown that not only the stiffness but also the viscosity of the environment regulates cell function.[71] Regarding cytotoxic lymphocytes such as T cells and NK cells, the combined effect of stiffness, viscosity, and additional physical factors on their immune function is still to be explored. Our work exposes what seems to be "the tip of the iceberg" of the physical sensing of NK cells. This sense undoubtedly deserves further investigation, as it will help understand the mechanism of the immune activity of NK cells, which is both fundamentally important and can facilitate the development of future immunotherapies.

ASSOCIATED CONTENT

Supporting Information

The Supporting Information is available free of charge at https://pubs.acs.org/doi/10.1021/acsbiomaterials.0c01121.

Additional experimental details and data, including measurements of PDMS stiffness, assessment of MICA density using fluorescence, activation of NK cells, control experiment with cytoskeletal inhibitors, quantification of NK cell response to inert surface chemistry, spreading of NK cells, quantification of NKG2D expression, quantification of DAP10 clustering, and a proposed model for NKG2D mechanosensing (PDF)

AUTHOR INFORMATION

Corresponding Author

Mark Schvartzman − *Department of Materials Engineering and Ilse Katz Institute for Nanoscale Science & Technology, Ben-Gurion University of the Negev, 84105 Beer Sheva, Israel*; orcid.org/0000-0002-5912-525X; Email: marksc@bgu.ac.il

Authors

Lital Mordechay − *Department of Materials Engineering and Ilse Katz Institute for Nanoscale Science & Technology, Ben-Gurion University of the Negev, 84105 Beer Sheva, Israel*

https://dx.doi.org/10.1021/acsbiomaterials.0c01121
ACS Biomater. Sci. Eng. 2021, 7, 122−132

Guillaume Le Saux − *Department of Materials Engineering and Ilse Katz Institute for Nanoscale Science & Technology, Ben-Gurion University of the Negev, 84105 Beer Sheva, Israel*
Avishay Edri − *The Shraga Segal Department of Microbiology, Immunology and Genetics, Faculty of Health Sciences, Ben-Gurion University of the Negev, 84105 Beer Sheva, Israel*
Uzi Hadad − *Ilse Katz Institute for Nanoscale Science & Technology, Ben-Gurion University of the Negev, 84105 Beer Sheva, Israel*
Angel Porgador − *The Shraga Segal Department of Microbiology, Immunology and Genetics, Faculty of Health Sciences, Ben-Gurion University of the Negev, 84105 Beer Sheva, Israel*

Complete contact information is available at: https://pubs.acs.org/10.1021/acsbiomaterials.0c01121

Author Contributions

The manuscript was written through contributions of all authors. All authors have given approval to the final version of the manuscript.

Notes

The authors declare no competing financial interest.

■ ACKNOWLEDGMENTS

This work was funded by the Multidisciplinary Research Grant - The Faculty of Health Science in Ben-Gurion University of the Negev and Israel Ministry of Science and Technology, Israel Science Foundation, Individual Grant #1401/15, and Israel Science Foundations: F.I.R.S.T. Individual Grant #2058/18. The authors thank Dr. Benyamin Rosental from The Shraga Segal Department of Microbiology, Immunology, and Genetics, Ben-Gurion University of the Negev, and Prof. Anne Bernhaim from the Department of Chemical Engineering, Ben-Gurion University of the Negev, for generous providing of cyosceleton inhibitors. The manuscript was written through contributions from all authors.

■ REFERENCES

(1) Vogel, V.; Sheetz, M. Local Force and Geometry Sensing Regulate Cell Functions. *Nat. Rev. Mol. Cell Biol.* **2006**, *7*, 265−275.
(2) Vogel, V.; Sheetz, M. P. Cell Fate Regulation by Coupling Mechanical Cycles to Biochemical Signaling Pathways. *Curr. Opin. Cell Biol.* **2009**, *21*, 38−46.
(3) Sheetz, M. P. Cell Control by Membrane-Cytoskeleton Adhesion. *Nat. Rev. Mol. Cell Biol.* **2001**, *2*, 392−396.
(4) Oria, R.; Wiegand, T.; Escribano, J.; Elosegui-Artola, A.; Uriarte, J. J.; Moreno-Pulido, C.; Platzman, I.; Delcanale, P.; Albertazzi, L.; Navajas, D.; Trepat, X.; García-Aznar, J. M.; Cavalcanti-Adam, E. A.; Roca-Cusachs, P. Force Loading Explains Spatial Sensing of Ligands by Cells. *Nature* **2017**, *552*, 219−224.
(5) Gardel, M. L.; Schneider, I. C.; Aratyn-Schaus, Y.; Waterman, C. M. Mechanical Integration of Actin and Adhesion Dynamics in Cell Migration. *Annu. Rev. Cell Dev. Biol.* **2010**, *26*, 315−333.
(6) Basu, R.; Huse, M. Mechanical Communication at the Immunological Synapse. *Trends Cell Biol.* **2017**, *27*, 241−254.
(7) Batista, F. D.; Dustin, M. L. Cell: Cell Interactions in the Immune System. *Immunol. Rev.* **2013**, *25*, 7.
(8) Dustin, M. L.; Groves, J. T. Receptor Signaling Clusters in the Immune Synapse. *Annu. Rev. Biophys.* **2012**, *41*, 543−556.
(9) Hammer, J. A., III; Burkhardt, J. K. Controversy and Consensus Regarding Myosin II Function at the Immunological Synapse. *Curr. Opin. Immunol.* **2013**, *25*, 300−306.
(10) Le Floc'h, A.; Huse, M. Molecular Mechanisms and Functional Implications of Polarized Actin Remodeling at the T Cell Immunological Synapse. *Cell. Mol. Life Sci.* **2015**, *72*, 537−556.
(11) Kim, S. T.; Shin, Y.; Brazin, K.; Mallis, R. J.; Sun, Z.-Y. J.; Wagner, G.; Lang, M. J.; Reinherz, E. L. TCR Mechanobiology: Torques and Tunable Structures Linked to Early T Cell Signaling. *Front. Immunol.* **2012**, *3*, 76.
(12) Hong, J.; Ge, C.; Jothikumar, P.; Yuan, Z.; Liu, B.; Bai, K.; Li, K.; Rittase, W.; Shinzawa, M.; Zhang, Y.; Palin, A.; Love, P.; Yu, X.; Salaita, K.; Evavold, B. D.; Singer, A.; Zhu, C. A TCR Mechanotransduction Signaling Loop Induces Negative Selection in the Thymus. *Nat. Immunol.* **2018**, *19*, 1379−1390.
(13) Natkanski, E.; Lee, W.-Y.; Mistry, B.; Casal, A.; Molloy, J. E.; Tolar, P. B Cells Use Mechanical Energy to Discriminate Antigen Affinities. *Science* **2013**, *340*, 1587−1590.
(14) Wan, Z.; Zhang, S.; Fan, Y.; Liu, K.; Davey, A. M.; Zhang, H.; Han, W. B Cell Activation Is Regulated by the Stiffness Properties of the Substrate Presenting the Antigens. *J. Immunol.* **2013**, *190*, 4661−4675.
(15) Judokusumo, E.; Tabdanov, E.; Kumari, S.; Dustin, M. L.; Kam, L. C. Mechanosensing in T Lymphocyte Activation. *Biophys. J.* **2012**, *102*, L5−L7.
(16) Zeng, Y.; Yi, J.; Wan, Z.; Liu, K.; Song, P.; Chau, A.; Wang, F.; Chang, Z.; Han, W.; Zheng, W.; Chen, Y. H.; Xiong, C.; Liu, W. Substrate Stiffness Regulates B-Cell Activation, Proliferation, Class Switch, and T-Cell-Independent Antibody Responses in Vivo. *Eur. J. Immunol.* **2015**, *45*, 1621−1634.
(17) Saitakis, M.; Dogniaux, S.; Goudot, C.; Bufi, N.; Asnacios, S.; Maurin, M.; Randriamampita, C.; Asnacios, A.; Hivroz, C. Different TCR-Induced T Lymphocyte Responses Are Potentiated by Stiffness with Variable Sensitivity. *Elife* **2017**, *6*, 1−29.
(18) O'Connor, R. S.; Hao, X.; Shen, K.; Bashour, K.; Akimova, T.; Hancock, W. W.; Kam, L. C.; Milone, M. C. Substrate Rigidity Regulates Human T Cell Activation and Proliferation. *J. Immunol.* **2012**, *189*, 1330−1339.
(19) Pegram, H. J.; Andrews, D. M.; Smyth, M. J.; Darcy, P. K.; Kershaw, M. H. Activating and Inhibitory Receptors of Natural Killer Cells. *Immunol. Cell Biol.* **2011**, *89*, 216−224.
(20) Orange, J. S. Formation and Function of the Lytic NK-Cell Immunological Synapse. *Nat. Rev. Immunol.* **2008**, *8*, 713−725.
(21) Davis, D. M.; Chiu, I.; Fassett, M.; Cohen, G. B.; Mandelboim, O.; Strominger, J. L. The Human Natural Killer Cell Immune Synapse. *Proc. Natl. Acad. Sci. U. S. A.* **1999**, *96*, 15062−15067.
(22) Matalon, O.; Fried, S.; Ben-Shmuel, A.; Pauker, M. H.; Joseph, N.; Keizer, D.; Piterburg, M.; Barda-Saad, M. Dephosphorylation of the Adaptor LAT and Phospholipase C-g by SHP-1 Inhibits Natural Killer Cell Cytotoxicity. *Sci. Signaling* **2016**, *9*, 1−16.
(23) Le Saux, G.; Bar-Hanin, N.; Edri, A.; Hadad, U.; Porgador, A.; Schvartzman, M. Nanoscale Mechanosensing of Natural Killer Cells Is Revealed by Antigen-Functionalized Nanowires. *Adv. Mater.* **2019**, *31*, 1805954.
(24) Bufi, N.; Saitakis, M.; Dogniaux, S.; Buschinger, O.; Bohineust, A.; Richert, A.; Maurin, M.; Hivroz, C.; Asnacios, A. Human Primary Immune Cells Exhibit Distinct Mechanical Properties That Are Modified by Inflammation. *Biophys. J.* **2015**, *108*, 2181.
(25) Kawano, S.; Kojima, M.; Higuchi, Y.; Sugimoto, M.; Ikeda, K.; Sakuyama, N.; Takahashi, S.; Hayashi, R.; Ochiai, A.; Saito, N. Assessment of Elasticity of Colorectal Cancer Tissue, Clinical Utility, Pathological and Phenotypical Relevance. *Cancer Sci.* **2015**, *106*, 1232−1239.
(26) Paszek, M. J.; Zahir, N.; Johnson, K. R.; Lakins, J. N.; Rozenberg, G. I.; Gefen, A.; Reinhart-King, C. A.; Margulies, S. S.; Dembo, M.; Boettiger, D.; Hammer, D. A.; Weaver, V. M. Tensional Homeostasis and the Malignant Phenotype. *Cancer Cell* **2005**, *8*, 241−254.
(27) Hu, W.; Wang, G.; Huang, D.; Sui, M.; Xu, Y. Cancer Immunotherapy Based on Natural Killer Cells: Current Progress and New Opportunities. *Frontiers in Immunology*. Frontiers Media S.A. May 2019, 1205.

(28) Lambert, L. H.; Goebrecht, G. K. E.; De Leo, S. E.; O'Connor, R. S.; Nunez-Cruz, S.; De Li, T.; Yuan, J.; Milone, M. C.; Kam, L. C. Improving T Cell Expansion with a Soft Touch. *Nano Lett.* **2017**, *17*, 821−826.
(29) Dang, A. P.; De Leo, S.; Bogdanowicz, D. R.; Yuan, D. J.; Fernandes, S. M.; Brown, J. R.; Lu, H. H.; Kam, L. C. Enhanced Activation and Expansion of T Cells Using Mechanically Soft Elastomer Fibers. *Adv. Biosys.* **2018**, *2*, 1700167.
(30) Bauer, S.; Groh, V.; Wu, J.; Steinle, A.; Phillips, J. H.; Lanier, L. L.; Spies, T. Activation of NK Cells and T Cells by NKG2D, a Receptor for Stress-Inducible MICA. *Science* **1999**, *285*, 727−729.
(31) Wang, Z.; Volinsky, A. A.; Gallant, N. D. Crosslinking Effect on Polydimethylsiloxane Elastic Modulus Measured by Custom-Built Compression Instrument. *J. Appl. Polym. Sci.* **2014**, *131*, 41050.
(32) Howatt, G. N.; Breckenridge, R. G.; Brownlow, J. M. Fabrication of Thin Ceramic Sheets for Capacitors. *J. Am. Ceram. Soc.* **1947**, *30*, 237−242.
(33) Placet, V.; Delobelle, P. Mechanical Properties of Bulk Polydimethylsiloxane for Microfluidics over a Large Range of Frequencies and Aging Times. *J. Micromech. Microeng.* **2015**, *25*, 1−8.
(34) Leadley, S.; O'Hare, L.-A.; McMillan, C. *Surface Analysis of Silicones*; 2012.
(35) Cappella, B. *Mechanical Properties of Polymers Measured through AFM Force-Distance Curves*; 2016, DOI: 10.1007/978-3-319-29459-9.
(36) Heuzé, M. L.; Sankara Narayana, G. H. N.; D'Alessandro, J.; Cellerin, V.; Dang, T.; Williams, D. S.; Van Hest, J. C.; Marcq, P.; Mège, R.-M.; Ladoux, B. Myosin II Isoforms Play Distinct Roles in Adherens Junction Biogenesis. *Elife* **2019**, *8*, 1−30.
(37) Huff, J. The Airyscan Detector from ZEISS: Confocal Imaging with Improved Signal-to-Noise Ratio and Super-Resolution. *Nat. Methods* **2015**, *12*, i−ii.
(38) Kuddannaya, S.; Chuah, Y. J.; Lee, M. H. A.; Menon, N. V.; Kang, Y.; Zhang, Y. Surface Chemical Modification of Poly-(Dimethylsiloxane) for the Enhanced Adhesion and Proliferation of Mesenchymal Stem Cells. *ACS Appl. Mater. Interfaces* **2013**, *5*, 9777−9784.
(39) Bálint, Š.; Lopes, F. B.; Davis, D. M. A Nanoscale Reorganization of the IL-15 Receptor Is Triggered by NKG2D in a Ligand-Dependent Manner. *Sci. Signal.* **2018**, *11*, eaal3606.
(40) Goda, T.; Konno, T.; Takai, M.; Moro, T.; Ishihara, K. Biomimetic Phosphorylcholine Polymer Grafting from Polydimethylsiloxane Surface Using Photo-Induced Polymerization. *Biomaterials* **2006**, *27*, 5151−5160.
(41) Li, P.; Morris, D. L.; Willcox, B. E.; Steinle, A.; Spies, T.; Strong, R. K. Complex Structure of the Activating Immunoreceptor NKG2D and Its MHC Class I-like Ligand MICA. *Nat. Immunol.* **2001**, *2*, 443−451.
(42) Keydar, Y.; Le Saux, G.; Pandey, A.; Avishay, E.; Bar-Hanin, N.; Esti, T.; Bhingardive, V.; Hadad, U.; Porgador, A.; Schvartzman, M. Natural Killer Cells' Immune Response Requires a Minimal Nanoscale Distribution of Activating Antigens. *Nanoscale* **2018**, *10*, 14651.
(43) Aktas, E.; Kucuksezer, U. C.; Bilgic, S.; Erten, G.; Deniz, G. Relationship between CD107a Expression and Cytotoxic Activity. *Cell. Immunol.* **2009**, *254*, 149−154.
(44) Alter, G.; Malenfant, J. M.; Altfeld, M. CD107a as a Functional Marker for the Identification of Natural Killer Cell Activity. *J. Immunol. Methods* **2004**, *294*, 15−22.
(45) Mace, E. M.; Wu, W. W.; Ho, T.; Mann, S. S.; Hsu, H.-T.; Orange, J. S. NK Cell Lytic Granules Are Highly Motile at the Immunological Synapse and Require F-Actin for Post-Degranulation Persistence. *J. Immunol.* **2012**, *189*, 4870−4880.
(46) Rak, G. D.; Mace, E. M.; Banerjee, P. P.; Svitkina, T.; Orange, J. S. Natural Killer Cell Lytic Granule Secretion Occurs through a Pervasive Actin Network at the Immune Synapse. *PLoS Biol.* **2011**, *9*, No. e1001151.
(47) Andzelm, M. M.; Chen, X.; Krzewski, K.; Orange, J. S.; Strominger, J. L. Myosin IIA Is Required for Cytolytic Granule Exocytosis in Human NK Cells. *J. Exp. Med.* **2007**, *204*, 2285−2291.
(48) Ma, Y.; Poole, K.; Goyette, J.; Gaus, K. Introducing Membrane Charge and Membrane Potential to T Cell Signaling. *Front. Immunol.* **2017**, *8*, 1−11.
(49) Arima, Y.; Iwata, H. Effects of Surface Functional Groups on Protein Adsorption and Subsequent Cell Adhesion Using Self-Assembled Monolayers. *J. Mater. Chem.* **2007**, *17*, 4079−4087.
(50) Culley, F. J.; Johnson, M.; Evans, J. H.; Kumar, S.; Crilly, R.; Casasbuenas, J.; Schnyder, T.; Mehrabi, M.; Deonarain, M. P.; Ushakov, D. S.; Braud, V.; Roth, G.; Brock, R.; Köhler, K.; Davis, D. M. Natural Killer Cell Signal Integration Balances Synapse Symmetry and Migration. *PLoS Biol.* **2009**, *7*, No. e1000159.
(51) Vanherberghen, B.; Olofsson, P. E.; Forslund, E.; Sternberg-Simon, M.; Khorshidi, M. A.; Pacouret, S.; Guldevall, K.; Enqvist, M.; Malmberg, K.-J.; Mehr, R.; et al. Classification of Human Natural Killer Cells Based on Migration Behavior and Cytotoxic Response. *Blood* **2013**, *121*, 1326−1334.
(52) Guldevall, K.; Brandt, L.; Forslund, E.; Olofsson, K.; Frisk, T. W.; Olofsson, P. E.; Gustafsson, K.; Manneberg, O.; Vanherberghen, B.; Brismar, H.; Kärre, K.; Uhlin, M.; Önfelt, B. Microchip Screening Platform for Single Cell Assessment of NK Cell Cytotoxicity. *Front. Immunol.* **2016**, *7*, 119.
(53) Sherman, E.; Barr, V.; Manley, S.; Patterson, G.; Balagopalan, L.; Akpan, I.; Regan, C. K.; Merrill, R. K.; Sommers, C. L.; Lippincott-Schwartz, J.; Samelson, L. E. Functional Nanoscale Organization of Signaling Molecules Downstream of the T Cell Antigen Receptor. *Immunity* **2011**, *35*, 705−720.
(54) Mattila, P. K.; Feest, C.; Depoil, D.; Treanor, B.; Montaner, B.; Otipoby, K. L.; Carter, R.; Justement, L. B.; Bruckbauer, A.; Batista, F. D. The Actin and Tetraspanin Networks Organize Receptor Nanoclusters to Regulate B Cell Receptor-Mediated Signaling. *Immunity* **2013**, *38*, 461−474.
(55) Liu, D.; Peterson, M. E.; Long, E. O. The Adaptor Protein Crk Controls Activation and Inhibition of Natural Killer Cells. *Immunity* **2012**, *36*, 600−611.
(56) Abeyweera, T. P.; Merino, E.; Huse, M. Inhibitory Signaling Blocks Activating Receptor Clustering and Induces Cytoskeletal Retraction in Natural Killer Cells. *J. Cell Biol.* **2011**, *192*, 675−690.
(57) Hadad, U.; Thauland, T. J.; Martinez, O. M.; Butte, M. J.; Porgador, A.; Krams, S. M. NKp46 Clusters at the Immune Synapse and Regulates NK Cell Polarization. *Front. Immunol.* **2015**, *6*, 495.
(58) Pageon, S. V.; Cordoba, S. P.; Owen, D. M.; Rothery, S. M.; Oszmiana, A.; Davis, D. M. Superresolution Microscopy Reveals Nanometer-Scale Reorganization of Inhibitory Natural Killer Cell Receptors upon Activation of NKG2D. *Sci. Signal.* **2013**, *6*, ra62.
(59) Le Saux, G.; Schvartzman, M. Advanced Materials and Devices for the Regulation and Study of NK Cells. *Int. J. Mol. Sci.* **2019**, *20*, 646. MDPI AG February
(60) Loftus, C.; Saeed, M.; Davis, D. M.; Dunlop, I. E. Activation of Human Natural Killer Cells by Graphene Oxide-Templated Antibody Nanoclusters. *Nano Lett.* **2018**, *18*, 3282−3289.
(61) Delcassian, D.; Depoil, D.; Rudnicka, D.; Liu, M.; Davis, D. M.; Dustin, M. L.; Dunlop, I. E. Nanoscale Ligand Spacing Influences Receptor Triggering in T Cells and NK Cells. *Nano Lett.* **2013**, *13*, 5608−5614.
(62) Le Saux, G.; Edri, A.; Keydar, Y.; Hadad, U.; Porgador, A.; Schvartzman, M. Spatial and Chemical Surface Guidance of NK Cell Cytotoxic Activity. *ACS Appl. Mater. Interfaces* **2018**, *10*, 11486−11494.
(63) Garrity, D.; Call, M. E.; Feng, J.; Wucherpfennig, K. W. The Activating NKG2D Receptor Assembles in the Membrane with Two Signaling Dimers into a Hexameric Structure. *Proc. Natl. Acad. Sci. U. S. A.* **2005**, *102*, 7641−7646.
(64) Quatrini, L.; Molfetta, R.; Zitti, B.; Peruzzi, G.; Fionda, C.; Capuano, C.; Galandrini, R.; Cippitelli, M.; Santoni, A.; Paolini, R. Ubiquitin-Dependent Endocytosis of NKG2D-DAP10 Receptor Complexes Activates Signaling and Functions in Human NK Cells. *Sci. Signal.* **2015**, *8*, ra108.
(65) Depoil, D.; Dustin, M. L. Force and Affinity in Ligand Discrimination by the TCR. *Trends Immunol.* **2014**, *35*, 597−603.

(66) Liu, B.; Chen, W.; Evavold, B. D.; Zhu, C. Accumulation of Dynamic Catch Bonds between TCR and Agonist Peptide-MHC Triggers T Cell Signaling. *Cell* **2014**, *157*, 357−368.
(67) Das, D. K.; Feng, Y.; Mallis, R. J.; Li, X.; Keskin, D. B.; Hussey, R. E.; Brady, S. K.; Wang, J.-H.; Wagner, G.; Reinherz, E. L.; Lang, M. J. Force-Dependent Transition in the T-Cell Receptor β-Subunit Allosterically Regulates Peptide Discrimination and PMHC Bond Lifetime. *Proc. Natl. Acad. Sci.* **2015**, *112*, 1517−1522.
(68) Hong, J.; Persaud, S. P.; Horvath, S.; Allen, P. M.; Evavold, B. D.; Zhu, C. Force-Regulated In Situ TCR−Peptide-Bound MHC Class II Kinetics Determine Functions of $CD4^+$ T Cells. *J. Immunol.* **2015**, *195*, 3557−3564.
(69) Pullen, R. H., III; Abel, S. M. Catch Bonds at T Cell Interfaces: Impact of Surface Reorganization and Membrane Fluctuations. *Biophys. J.* **2017**, *113*, 120−131.
(70) González, C.; Chames, P.; Kerfelec, B.; Baty, D.; Robert, P.; Limozin, L. Nanobody-CD16 Catch Bond Reveals NK Cell Mechanosensitivity. *Biophys. J.* **2019**, *116*, 1516−1526.
(71) Chaudhuri, O.; Gu, L.; Klumpers, D.; Darnell, M.; Bencherif, S. A.; Weaver, J. C.; Huebsch, N.; Lee, H. P.; Lippens, E.; Duda, G. N.; Mooney, D. J. Hydrogels with Tunable Stress Relaxation Regulate Stem Cell Fate and Activity. *Nat. Mater.* **2016**, *15*, 326−334.

https://dx.doi.org/10.1021/acsbiomaterials.0c01121
ACS Biomater. Sci. Eng. 2021, 7, 122−132